Electronic Supplementary Material (ESI) for Journal of Materials Chemistry B.

Supplementary

Fabrication of Photo-electrochemical biosensor for ultrasensitive screening of mono-bioactive molecules: effect of geometrical structures and crystal surfaces

N. Akhtar[a,b], M.Y. Emran[a], M. A. Shenashen[a], , T. Osaka [b], A. Faheem [c], T. Homma [b], H. Kawarada [b*], S. A. El-Safty[a,*]

Characterization analyses

The morphologies of the annealed samples were investigated by FE-SEM (JEOL Model 6500) at 20 kV. Analysis material was fixed onto the FE-SEM stage using carbon tape before insertion into the FE-SEM chamber. The ion sputter (Hitachi E-1030) was used to deposit thin-layered Pt films on electrodes at 25 °C.

A focused ion beam (FIB) system (JEM-9320FIB) operated at accelerating voltages from 5–30 kV with variable steps of 5 kV and magnification ranging from 150× to 300000×. The orientation axis (X and Y) of the powder samples containing NiO with different morphological structures CN-ST can be changed within ±1.2 mm through a tilt angle of ± 60°. The samples were inserted inside the FIB machine using a bulk-sample holder (8 × 8 mm^2) after deposition by a carbon protection layer. Before FIB investigation, the powder samples of the NiO with different morphological structures CN-ST were mixed with small amounts of epoxy (Gatan, Inc.) onto a small silicon wafer using a fine eyelash probe to form very thin films on the silicon. Each thin film was backed on a hot plate at 130 °C for 10 min and subsequently coated with a uniformly thin carbon layer of about 30 nm. The samples were inserted into the FIB microscope operated at 30 kV and then roughly milled on both sides until a final thickness of 2 μm using −1.5° and +1.5° tilts. Afterward, the NiO with different morphological structures CN-ST were cut and removed from the FIB system for subsequent HR-SEM analysis.

High-resolution transmission electron microscopy (HRTEM), electron diffraction (ED), scanning transmission electron microscopy (STEM), and energy dispersive X-ray spectroscopy for elemental mapping (STEM-EDS) were performed using a JEOL JEM model 2100F microscope. HRTEM was conducted at an acceleration voltage of 200 kV to obtain a lattice resolution of 0.1 nm and the spherical aberration of 1.0 mm. The HRTEM, STEM and STEM-EDS were operated at a camera length of 20 and a spot size of 1 nm. STEM and STEM-EDS were carried out at a camera length of 40 cm and a spot size of 0.7 nm. In the HRTEM, ED,

STEM, and STEM-EDS characterization, the samples were dispersed in ethanol solution using an ultrasonic cleaner, and then dropped on a copper grid. Prior to inserting the samples into the HRTEM column, the grid was vacuum dried for 20 min.

The surface properties of the material involving the pore structure distribution and surface area were estimated by N_2 adsorption–desorption isotherms at 77 K using a BELSORP36 analyzer (JP. BEL Co., Ltd.). The samples were thermally treated at 200 °C for at least 6 h under N_2 atmosphere. The specific surface area (S_{BET}) was calculated using the Brunauer–Emmett–Teller (BET) method with multipoint adsorption data from the linear section of the N_2 adsorption isotherm. The pore size distribution was determined using nonlocal DFT (NLDFT).

The structural geometry of the catalysts was further examined by WA-XRD. The WA-XRD patterns were recorded using a 18 kW diffractometer (Bruker D8 Advance) at scan rate of 10°/min with monochromated CuKα-X-radiation (λ = 1.54178 Å). The DIFRAC plus Evaluation Package (EVA) software with the PDF-2 Release 2009 databases provided by Bruker AXS was used to analyze the diffraction and structure analysis diffraction data. The TOPAS package program was applied to integrate various types of X-ray diffraction (XRD) analyses.

XPS analysis was conducted on a PHI Quantera SXM (ULVAC-PHI) instrument (Perkin–Elmer Co., USA) equipped with Al Kα as an X-ray source for excitation (1.5 mm × 0.1 mm, 15 kV, 50 W) under a pressure of 4×10^{-8} Pa. A thin film of the sample was deposited on a Si slide before the start of analysis.

Raman spectroscopy (HR Micro Raman spectrometer, Horiba, Jobin Yvon) was conducted using an Ar ion laser at 633 nm. A CCD (charge coupled device) camera detection system and the LabSpec-3.01C software package were used for data acquisition and analysis, respectively. To ensure the accuracy and precision of the Raman spectra, 10 scans of 5 s from 300 cm^{-1} to 1,600 cm^{-1} were recorded.

Scheme S1. The schematic synthesis approach of SST, DST and AST within addition of 15 mL of 1 Mm $(NH_4)_2HPO_4$ with controllable rate (Q).

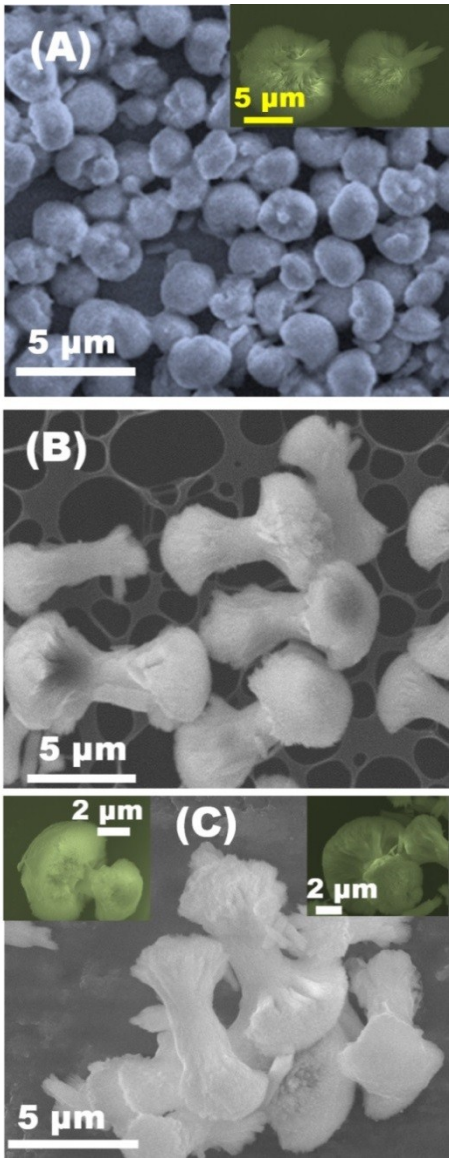

Figure S1 A) low magnification of FE-SEM shows the morphology of CN-SST which is like spear thistle (ST) with head and trunk, inset; high magnification FE-SEM of CN-SST. B) FE-SEM micrograph of ST with two symmetric head connected by rod in-between (CN-DST). C) Low magnification of FE-SEM obtains the ST morphology which is like a spear thistle (ST) with two asymmetric head, and its inset high magnification of CN-AST unit.

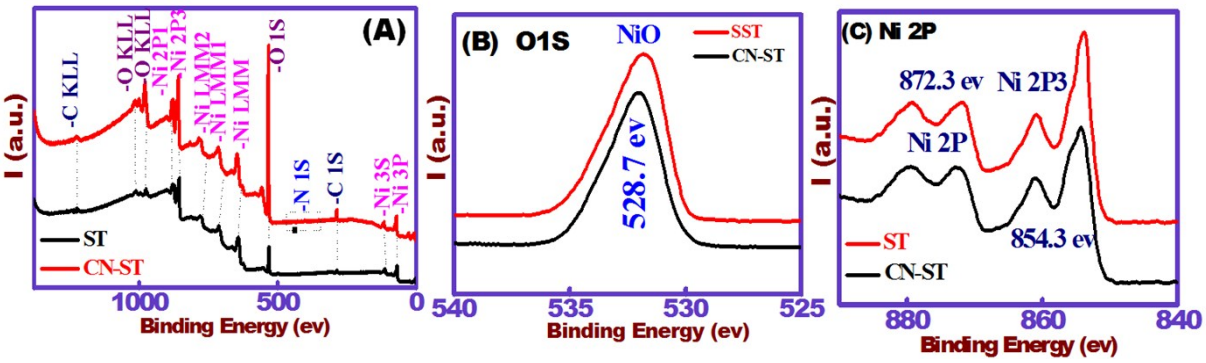

Figure S2. (A) XPS spectra of ST and CN-ST, Survey of the samples; (B) O 1S and (C) Ni 2P.

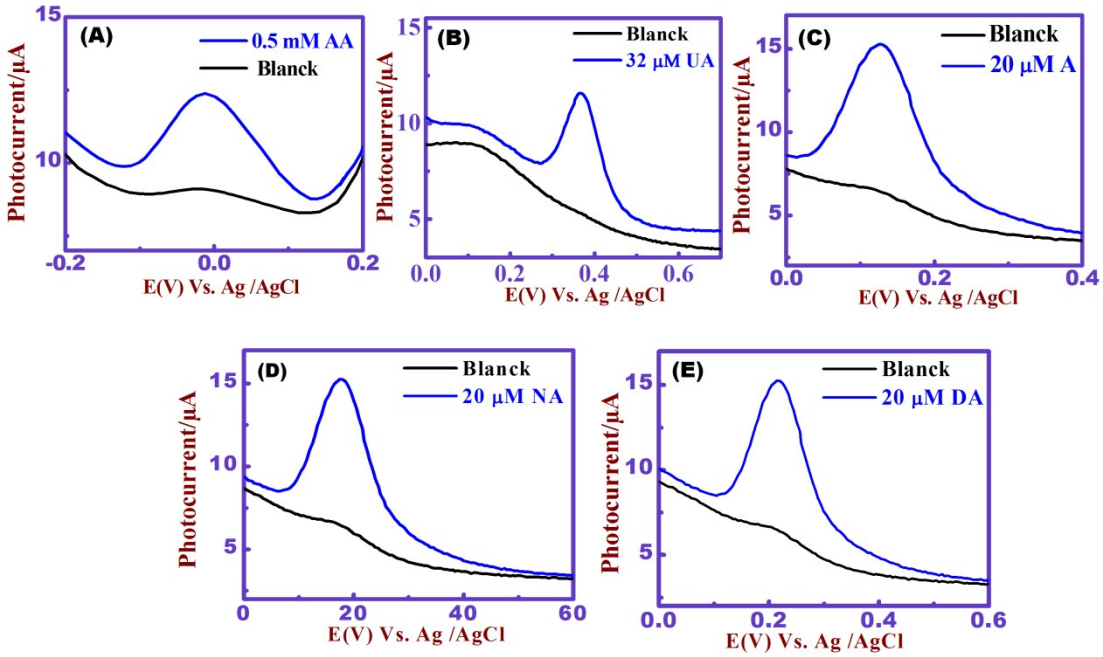

Figure S3. DPV of 0.5 mM AA (a), 32 μM UA(b), 20 μM A(c), 20 μM NA(d) and 20 μM DA (e) at CN-SST photo-biosensor electrode under UV light irradiation (365 nm) in 0.1 M PBS pH=7.4.

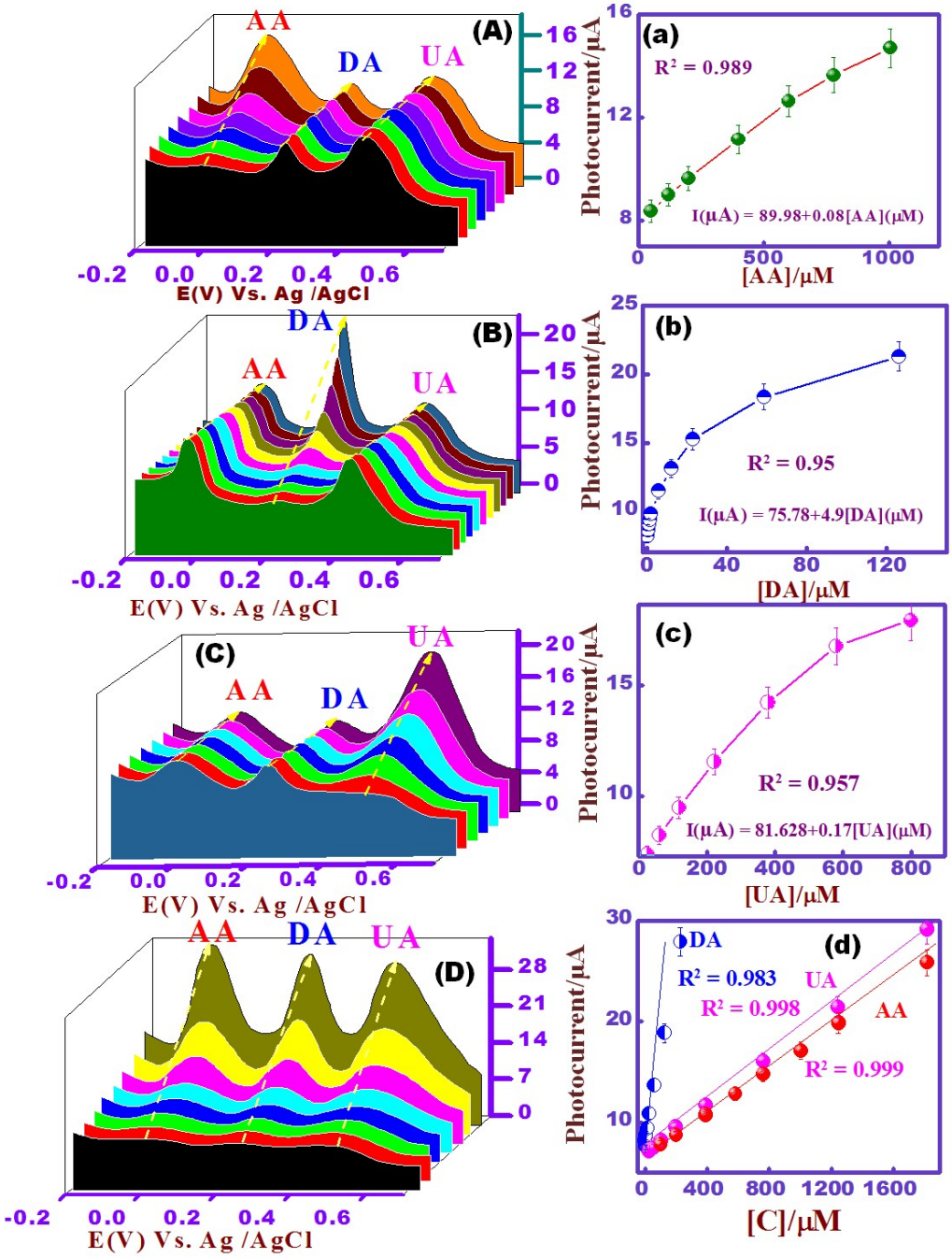

Figure S4. DPV curves at, (A) increasing concentrations of AA (50-1000 μM) in the presence of 10 μM DA and 0.2 mM UA (a) the plot of concentration of AA (μM) versus current (μA) , (B) increasing concentrations of DA (0.1-125 μM) in the presence of 0.5 mM AA and 0.2 mM UA, (b) the plot of concentration of DA (μM) versus current (μA), (C) increasing concentrations of UA (25-800 μM) in the presence of 10 μM DA and 0.5 mM AA, (c) the plot of concentration of DA (μM) versus current (μA) and (D) increasing concentrations of AA (25-1800 μM), DA (2-225 μM) and UA (100-1800 μM), (d) the plot of concentration of AA, DA and UA (μM) versus current (μA) simultaneously under UV light irradiation (365 nm) in 0.1 M PBS (pH 7.4) on CN-SST photo-biosensor electrode.

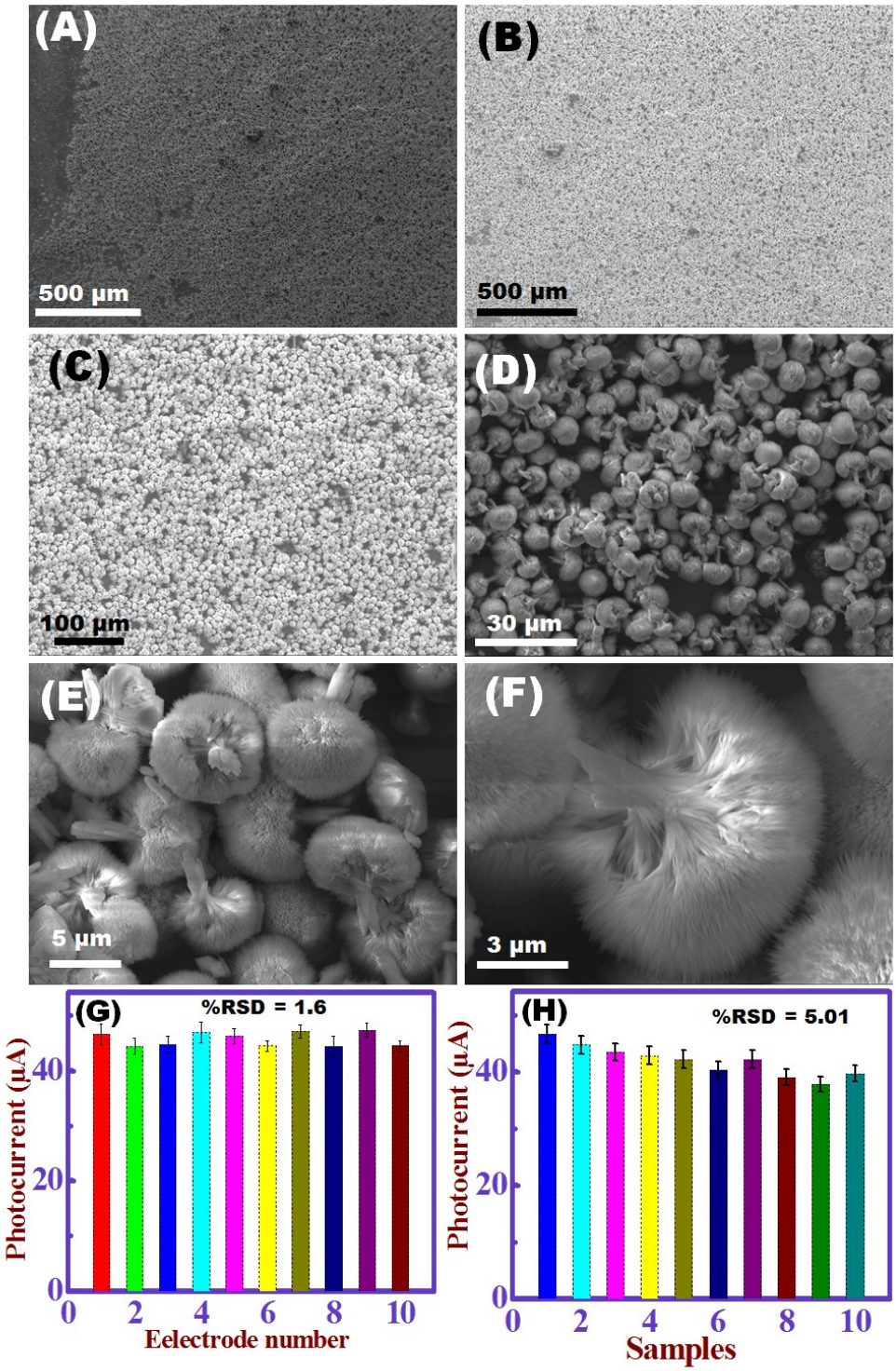

Figure S5. A-C) FE-SEM images of CN-SST at ITO glass substrate after 20 cyclic voltammograme cycles in 0.1 M PBS (pH 7.4) containing 0.5 mM DA. D-F) High magnification of FE-SEM was focused on the CN-SST unit for clearing the structure stability for each unity after using the photo-biosensor electrode in 0.5 mM DA. G) The columns of the reproducibility of CN-SST photo-biosensor electrode of 10 different electrodes to 5 µM DA. H) The column plot of the reusability of CN-SST photo-biosensor electrode for 10 samples with constant concentration of DA (5 µM) µm under UV light irradiation (365 nm) in PBS pH=7.4.

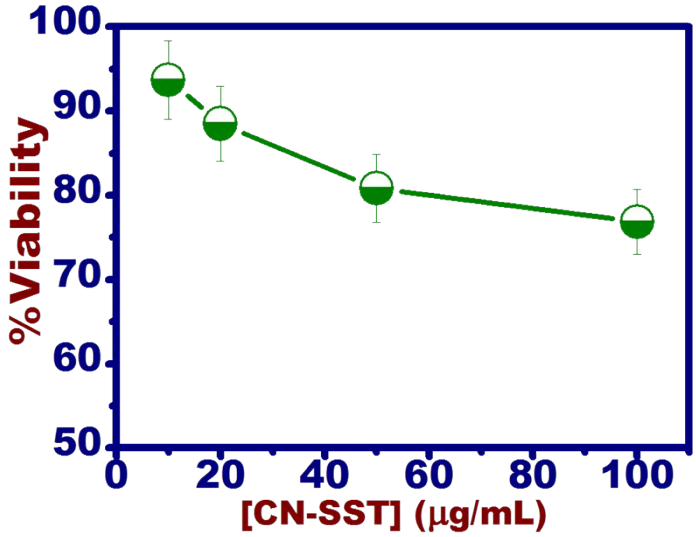

Figure S6. The effect of CN-SST concentrations (μg/mL) on the cell viability of PC12 cell line by CCK-8 assay using microplate reader at 450 nm after incubation of each concentration for 48 h.

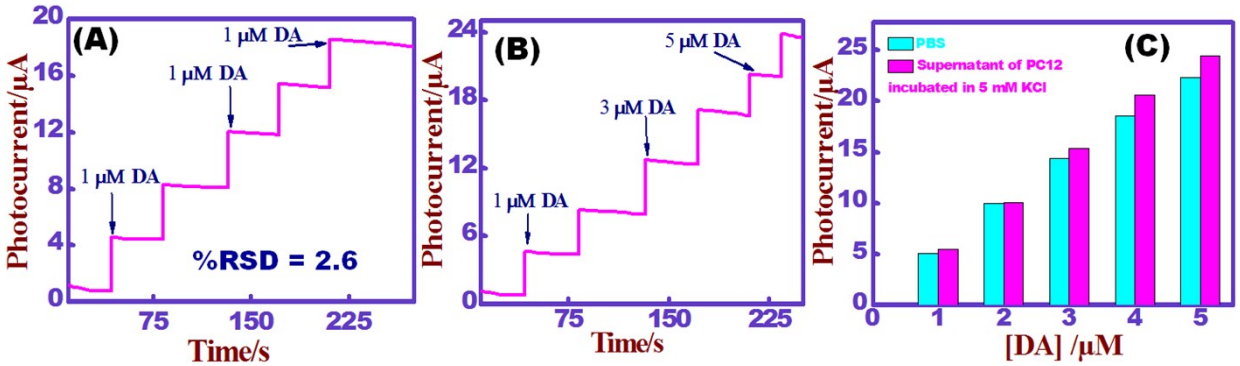

Figure S7. Amperometric response of dopamine addition in PBS pH=7.4 without (A) and with PC 12 induced by 5 mM KCl (B). The column plot represents the concentration of dopamine with (magenta column) and without (cyan column) PC12 (5 mM KCl) Vs the photocurrent current (μA) under UV light irradiation on CN-SST photo-biosensor electrode.

Table S1. The quantitative analyses of DA were carried out by spiking it with concentration in the range of 1-5 µmol L^{-1} on CN-SST photo-biosensor electrode into 0.1 M PBS (pH 7.4) containing human serum. The standardization analyses of targets were determined according to amperometric techniques at 0.21 V, and repeated 3 times per each sample analysis.

Sample	DA[a] added µM/L^{-1}	DA[b] found µM/L^{-1}	%R[c]
Serum sample	1	1.16± 0.001	116
	2	2.37± 0.003	118
	3	3.08± 0.005	102.6
	4	3.88± 0.001	97
	5	4.99± 0.002	99.8

[a] Dopamine added to the serum sample samples (C_A).

[b] Dopamine founded at the presented calibration curve (C_F).

[c] %Recovery is the percentage of recovery (%R= C_A/C_F x 100)